Nuclear Science and Techniques (2024) 35:77
https://doi.org/10.1007/s41365-024-01453-x

Stepped-up development of accelerator mass spectrometry method for the detection of ^{60}Fe with the HI-13 tandem accelerator

Yang Zhang[1] · Sheng-Quan Yan[1] · Ming He[1] · Qing-Zhang Zhao[1] · Wen-Hui Zhang[1] · Chao-Xin Kan[1] · Jian-Ming Zhou[1] · Kang-Ning Li[1] · Xiao-Fei Wang[1] · Jian-Cheng Liu[1] · Zhao-Hua Peng[1] · Zhuo Liang[1] · Ai-Ling Li[1] · Jian Zheng[1] · Qi-Wen Fan[1] · Yun-Ju Li[1] · You-Bao Wang[1] · Zhi-Hong Li[1] · Yang-Ping Shen[1] · Ding Nan[1] · Wei Nan[1] · Yu-Qiang Zhang[1] · Jia-Ying-Hao Li[1] · Jun-Wen Tian[1] · Jiang-Lin Hou[1] · Chang-Xin Guo[1] · Zhi-Cheng Zhang[1] · Ming-Hao Zhu[1] · Yu-Wen Chen[1] · Yu-Chen Jiang[1] · Tao Tian[1] · Jin-Long Ma[1] · Yi-Hui Liu[1] · Jing-Yu Dong[1] · Run-Long Liu[1] · Mei-Yue-Nan Ma[1] · Yong-Shou Chen[1] · Wei-Ping Liu[1,2] · Bing Guo[1,3]

Received: 23 January 2024 / Revised: 27 March 2024 / Accepted: 1 April 2024 / Published online: 24 May 2024

Abstract

The Moon provides a unique environment for investigating nearby astrophysical events such as supernovae. Lunar samples retain valuable information from these events, via detectable long-lived "fingerprint" radionuclides such as ^{60}Fe. In this work, we stepped up the development of an accelerator mass spectrometry (AMS) method for detecting ^{60}Fe using the HI-13 tandem accelerator at the China Institute of Atomic Energy (CIAE). Since interferences could not be sufficiently removed solely with the existing magnetic systems of the tandem accelerator and the following Q3D magnetic spectrograph, a Wien filter with a maximum voltage of ± 60 kV and a maximum magnetic field of 0.3 T was installed after the accelerator magnetic systems to lower the detection background for the low abundance nuclide ^{60}Fe. A 1 μm thick Si_3N_4 foil was installed in front of the Q3D as an energy degrader. For particle detection, a multi-anode gas ionization chamber was mounted at the center of the focal plane of the spectrograph. Finally, an ^{60}Fe sample with an abundance of 1.125×10^{-10} was used to test the new AMS system. These results indicate that ^{60}Fe can be clearly distinguished from the isobar ^{60}Ni. The sensitivity was assessed to be better than 4.3×10^{-14} based on blank sample measurements lasting 5.8 h, and the sensitivity could, in principle, be expected to be approximately 2.5×10^{-15} when the data were accumulated for 100 h, which is feasible for future lunar sample measurements because the main contaminants were sufficiently separated.

Keywords Accelerator mass spectrometry · Wien filter · Isobar separation · Supernovae · Chang'e-5 lunar samples

Yang Zhang and Sheng-Quan Yan have contributed equally to this work.

This work was supported by the National Natural Science Foundation of China (Nos. 12125509, 12222514, 11961141003, and 12005304), National Key Research and Development Project (No. 2022YFA1602301), CAST Young Talent Support Plan, the CNNC Science Fund for Talented Young Scholars Continuous support for basic scientific research projects.

✉ Bing Guo
guobing@ciae.ac.cn

1 China Institute of Atomic Energy, P.O. Box 275(10), Beijing 102413, China

2 College of Science, Southern University of Science and Technology, Shenzhen 518055, China

3 School of Physics, Xi'an Jiaotong University, Xi'an 710049, China

1 Introduction

The Moon is an excellent location for the storage of interstellar dust. There have been no geological or biological activities for more than a billion years [1–5], except for some mild gardening processes such as micrometeorite bombardment [6]. The dust deposited on the surface of the Moon contains long-lived radionuclides such as ^{60}Fe ($t_{1/2} = 2.61 \pm 0.04$ My [7, 8]), which are mainly produced in massive stars and ejected by supernova explosions [9–11] while cosmic rays produce a small amount [12]. Therefore, ^{60}Fe can provide evidence for tracing the passing of ejecta of nearby supernova events that have occurred within the last several million years. However, the ^{60}Fe/Fe ratio of lunar samples is approximately 10^{-15} [12], which falls below the detection

limit of most nuclide analytical methods. Accelerator mass spectrometry is the only method capable of detecting ^{60}Fe. This method was employed to determine the abundance of ^{60}Fe in deep-sea ferromanganese crusts [13, 14], marine sediments [15], Antarctic snow [16] and lunar soils brought back by the Apollo and Luna programs [12].

Chang'e-5 has completed China's first sample-gathering lunar mission, acquiring scooped and drilled samples from the northeastern Oceanus Procellarum on the Moon at longitudes and latitudes of 51.916 °W and 43.058 °N. This latitude is considerably higher than that of earlier sample collection sites of Apollo and Luna, which ranged from −8.973 °N to 26.133 °N. Hence, the new samples from the Chang'e-5 mission may provide more information (such as lunar petrology and volcanism [17–20], lunar geochemistry [21–23], and lunar soil maturity [24]). Motivated by this goal, we stepped up the development of the AMS facility at the China Institute of Atomic Energy to detect ^{60}Fe in lunar samples.

2 AMS setup

The HI-13 tandem accelerator at CIAE was accepted from the HVEC in 1986 and commenced full operations in early 1988 [25, 26]. AMS measurements based on this accelerator began in 1989 [27]. Nuclides such as ^{10}Be, ^{32}Si, ^{36}Cl, ^{41}Ca have been measured using this facility [28–31].

A schematic diagram of the AMS setup is illustrated in Fig. 1. The injection system was specifically designed for AMS measurements, featuring an NEC multi-cathode source of negative ions by Cs sputtering (MC-SNICS), which can accommodate up to forty cathodes. Negative ion beams are first filtered using a 90° electrostatic analyzer and a 112° injection magnet. Retractable Faraday cups are placed after each magnet to measure the beam current. Two offset Faraday cups are installed at the focal plane of the injection magnet. A gaussmeter is mounted inside the injection magnet to ensure reproducibility.

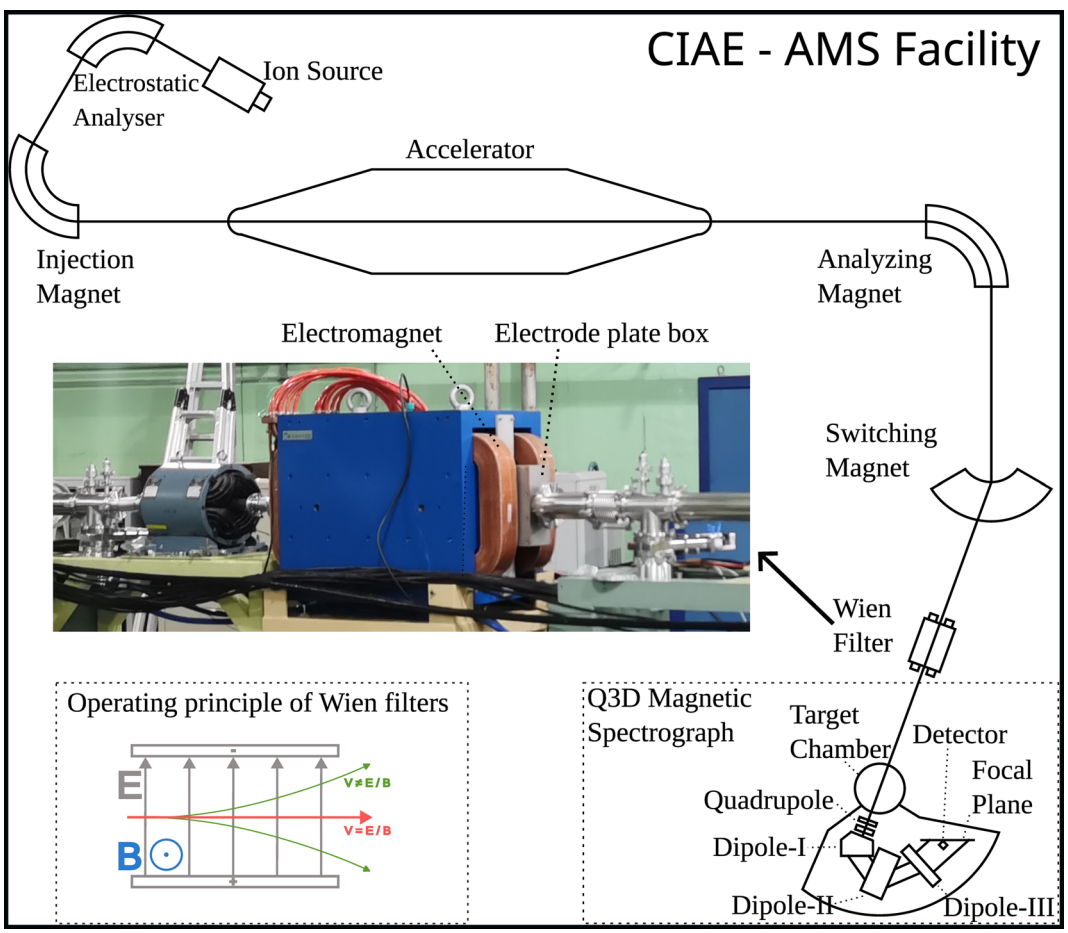

Fig. 1 (Color online) Diagram of the HI-13 tandem accelerator AMS system at the CIAE, featuring a photograph of the installed Wien filter, along with a quadrupole doublet placed in front of it. Only major parts are drawn and most of the beam-guiding devices are not displayed. There is a retractable target holder at the center of the target chamber, which was installed with the Si_3N_4 degrader

The HI-13 tandem accelerator can reach an approximate 12.5 MV terminal voltage and is capable of foil and gas stripping. Following the accelerator, an analyzing magnet and a switching magnet are present. The analyzing magnet has a mass energy product of 200 amu·MeV (mE/Z^2). The terminal component of the AMS beamline is a Q3D magnetic spectrograph that sequentially comprises a target chamber, a quadrupole, three dipoles, and a focal plane. A Si_3N_4 foil was installed in the target chamber as an energy degrader for additional isobar separation. The magnetic spectrograph has exhibited an energy resolution of 2×10^{-4} and a dispersion along the focal plane, determined by the least squares fit, of 11.37 (cm/1%$\Delta P/P$) [32]. A multi-anode gas ionization chamber (four anodes in this work) with an entrance window of 65 mm × 40 mm was mounted at the center of the focal plane for particle detection. The ΔE-Q3D detection method is developed with this system for isobar identification. Detailed descriptions of the ΔE-Q3D method have been reported [33, 34].

Despite the high sensitivity of the described AMS system, the contaminants in the beam of rare ions of interest cannot be completely removed by the high-resolution magnetic systems of the tandem accelerator. This limitation can lead to detector saturation in certain cases, such as in ^{60}Fe measurements. To address this issue, a Wien filter was installed after the switching magnet to reduce the interfering beams entering the final detector along with the rare ions of interest. The Wien filter is discussed in detail in the subsequent section.

2.1 Beam purification with Wien filter

A Wien filter utilizes orthogonal electric and magnetic fields to selectively influence the ions within a beam. Only ions with a specific velocity pass unaffectedly, whereas ions with different velocities are deflected by the electromagnetic force and subsequently blocked. A Wien filter manufactured by Danfysik was installed to purify the beam before it entered the Q3D magnetic spectrograph. The maximum voltage of the Wien filter is ±60 kV, and the maximum magnetic field is 0.3 T. The Wien filter parameters are listed in Table 1. A quadrupole doublet was positioned in front of the Wien filter to focus the beam at the entrance of the Q3D magnetic spectrograph. A slit was added 2 m from the Wien filter exit to block the deflected and defocused interfering beams. A collimator with a diameter of 5 mm can also be used for this purpose.

A test experiment with an ^{58}Fe beam was performed to evaluate the performance of the Wien filter. During this experiment, the analyzing and switching magnets were optimized for the transmission of ^{58}Fe. A multi-anode gas ionization chamber was mounted on the focal plane of the Q3D for detection. The energy-loss spectra for the first anode E_1 versus the total energy E_{total} are illustrated in Fig. 2. When the Wien filter was not activated, there was a significant presence of interfering beams, as illustrated in Fig. 2a. Most contaminants were suppressed by the Wien filter when the parameters were optimized for ^{58}Fe as illustrated in Fig. 2b. Small numbers of ions with the same m/q and E/q as the ions of interest also enter the detector. However, they were sufficiently separated in the energy spectra. In this experiment, the magnetic field of the Q3D was optimized for the tail of the ^{58}Fe because of the high counting rate of the ^{58}Fe beam.

Table 1 Parameters of the Wien filter

Parameter	Value
Max. magnetic field (T)	0.3
Effective magnetic length (mm)	1032
Polo gap (mm)	140
Max. electrical field (kV cm^{-1})	24
Effective electrical length (mm)	1080
Max. electrodes voltage (kV)	60
Electrode gap (mm)	50
Electrode width (mm)	80

2.1.1 Isobar suppression

The abundance of ^{60}Fe in lunar samples is extremely low, with ^{60}Fe/Fe estimated at the level of 10^{-15}. Separating ^{60}Fe from ^{60}Ni using most electromagnetic devices is challenging due to the isobar ^{60}Ni having nearly the same mass. ^{60}Fe and ^{60}Ni have to be separated at high energies by the dE/dx method; however, excessive ^{60}Ni mixed in the ^{60}Fe beam would saturate the data acquisition system. Hence, ^{60}Ni must be reduced during each step of the AMS measurement.

First, to reduce the influence of the ^{60}Ni, the samples used for ^{60}Fe measurements were chemically treated to reduce Ni using a solvent extraction method and an anion-exchange step. Second, copper powder with a relatively high purity of 99.999% was mixed with the ^{60}Fe samples (in the form of Fe_2O_3 powder) in an approximately 1:1 weight ratio to increase the beam current at the ion source of the accelerator. Third, the ion extracted for ^{60}Fe measurements was $^{60}FeO^-$, which produced a stronger beam current and higher ^{60}Fe/^{60}Ni ratio than $^{60}Fe^-$ [35]. The holders of the samples in the ion source are composed of high-purity copper.

Although the aforementioned methods significantly reduced the nickel content, the remaining ^{60}Ni could not be separated by electromagnetic devices and remained beyond the capacity of the data acquisition system. Thus, aided by an energy degrader foil, the ΔE-Q3D [33, 34] method was employed to separate ^{60}Ni from ^{60}Fe before

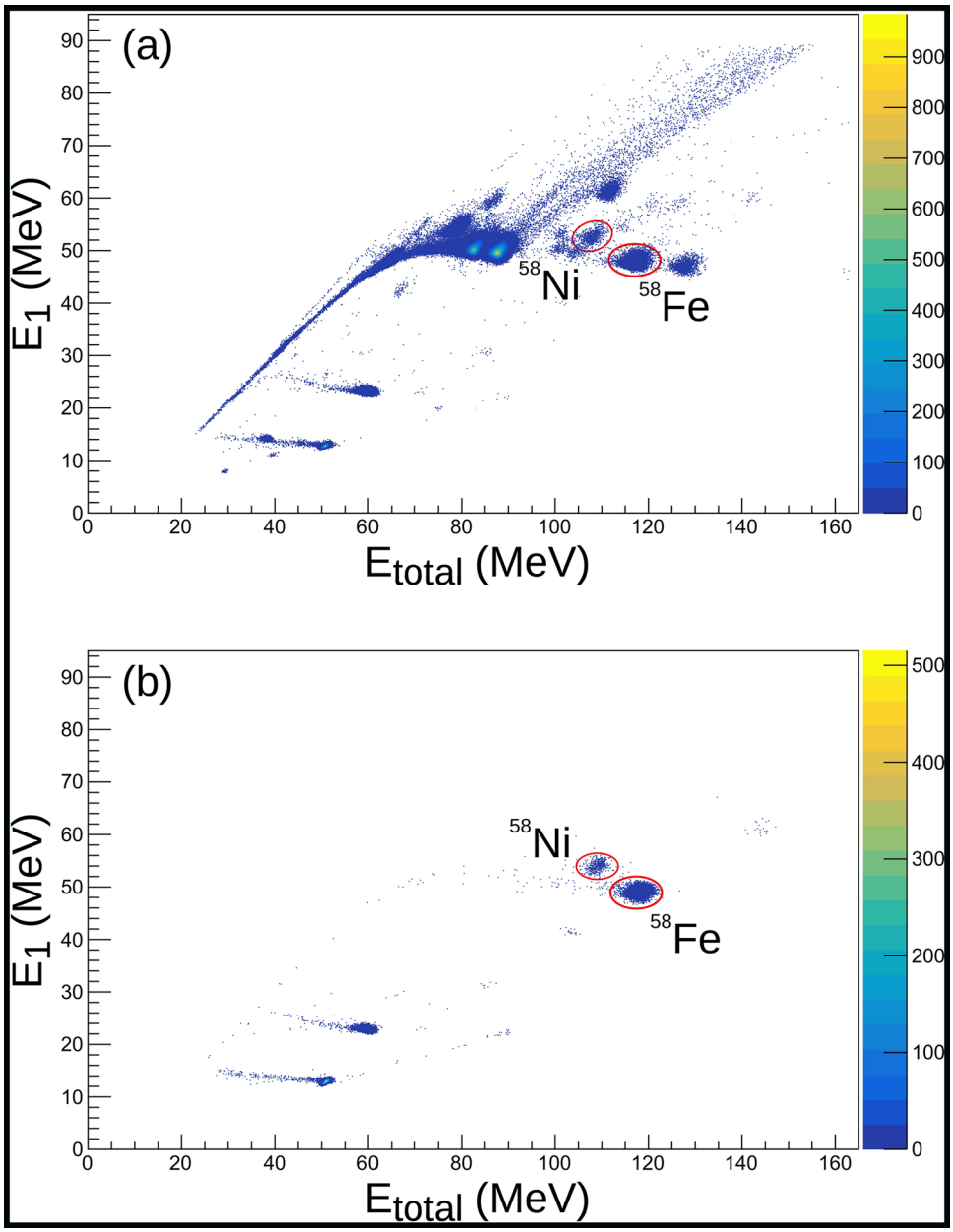

Fig. 2 (Color online) Two-dimensional spectra of E_1 versus E_{total}. E_1 is the energy loss of the first anode, and E_{total} is the total energy of the ions in the detector. **a** Spectrum measured without the Wien filter. **b** Spectrum measured with the Wien filter of ±50 kV voltage and corresponding magnetic field. The areas for ^{58}Fe and ^{58}Ni are marked by red circles

entering the final detector, because the energies of ^{60}Fe and ^{60}Ni will be different after passing the foil. In this method, a highly homogeneous Si_3N_4 foil with a thickness of 1 μm was installed in the target chamber as an energy degrader. When ^{60}Fe and ^{60}Ni with energies of 130 MeV pass through the degrader, the energy difference is approximately 1 MeV, and the energy straggling is approximately 200 keV at FWHM. This difference is sufficient for the Q3D to separate ^{60}Ni from ^{60}Fe. Although several scattered ^{60}Ni ions entered the detector, the remaining intensities were low; ^{60}Fe and ^{60}Ni can be distinguished using a multi-anode gas ionization chamber.

2.1.2 Experimental procedure

The HI-13 tandem accelerator operated at a terminal voltage of 11 MV for the ^{60}Fe AMS measurements. Considering the stripping efficiency and beam energy, carbon foils with a thickness of 3 μg/cm^2 and charge state of 11^+ were selected. At this terminal voltage, the stripping efficiency is around 7%, and the beam energy is approximately 130 MeV.

As the ^{60}Fe ion flux cannot be measured using Faraday cups, it is necessary to simulate ^{60}Fe beam transport with another nearby nuclide. ^{59}Co was selected as a pilot beam instead of ^{60}Ni to avoid heavy contamination in subsequent measurements. The beam-guiding devices were optimized

to maximize the overall transmission efficiency. The transmission efficiency is calculated as follows:

$$\eta = \frac{I_{\mathrm{Q3D}}}{q \cdot I_{\mathrm{InjSys}}}, \tag{1}$$

where I_{InjSys} and I_{Q3D} are the beam currents measured with Faraday cups before the accelerator and ΔE-Q3D system, respectively; q is the charge of the ions. The efficiency was approximately 2 % in this experiment.

Initially, all the accelerator magnet parameters were optimized for the transmission of ^{59}CoO$^-$ to ^{59}Co^{11+}. To calibrate the Wien filter, the ^{59}Co beam was first measured using a Faraday cup in the target chamber without the Wien filter. Subsequently, the Wien filter parameters were optimized for ^{59}Co to reproduce the beam current. In ^{60}Fe measurements, the parameters of the Wien filter were optimized based on ^{59}Co. The slit after the Wien filter and collimator in the target chamber was used to block deflected contamination ions. To optimize the ^{60}Fe beam, the parameters of the major magnets, including the injection magnet, the analyzing magnet, switching magnet, and the Wien filter, were adjusted based on calculations. These parameters were fine-tuned based on the counting rate of the ^{60}Fe.

After the Si_3N_4 degrader, ^{60}Fe and ^{60}Ni were separated using Q3D. As the counting rate of ^{60}Fe was extremely low, initially, the magnets of the Q3D were optimized on ^{60}Ni to calibrate the parameters. The Q3D magnet parameters were then scaled to detect ^{60}Fe from the set previously tuned using ^{60}Ni. The optimized experimental parameters are listed in Table 2.

3 Results

In these measurements, an ^{60}Fe blank sample was initially measured. Subsequently, a sample with an ^{60}Fe abundance of 1.125×10^{-10} was used for testing. The results are presented in Fig. 3. E_1 and E_3 are the energy losses at the first and the third anode, respectively. ^{60}Fe is clearly distinguished from ^{60}Ni, as illustrated in Fig. 3b. In the spectra, a substantial amount of ^{60}Ni and a few other contaminants are present; however, they are far away from the region of ^{60}Fe and do not affect the identification. The sensitivity of AMS measurements, r, was calculated as

$$r = \frac{N_{\mathrm{blank}}/Q'}{N_{^{60}\mathrm{Fe}}/Q} \cdot r_{\mathrm{sample}}, \tag{2}$$

where N_{blank} and $N_{^{60}\mathrm{Fe}}$ are the event counts in the area for the ^{60}Fe of the blank sample and ^{60}Fe sample measurements, respectively. Q' and Q are the numbers of ^{58}Fe^{16}O$^-$ collected at the injection system for the blank sample and the ^{60}Fe sample measurements, respectively; r_{sample} is the abundance of the ^{60}Fe sample. In the measurements of the ^{60}Fe blank sample, data were accumulated for 5.8 h and the average current of ^{58}Fe^{16}O$^-$ was 40 enA. No ^{60}Fe events were detected in this area. 152 ^{60}Fe ion counts accumulated over 6 h, and the average current of ^{58}Fe^{16}O$^-$ was 2.2 enA. Consequently, the sensitivity of ^{60}Fe measurements in the test experiment was estimated to be better than 4.3×10^{-14}. The sensitivity could, in principle, be expected to be approximately 2.5×10^{-15} when the data are accumulated for 100 h. This, with the use of a pristine set of ion source components in the ionizer region, is feasible for accumulation over multiple cathodes for future lunar sample measurements because the main contaminants are sufficiently separated, as illustrated in Fig. 3b.

4 Conclusion and outlook

The AMS facility at the HI-13 tandem accelerator has been developed for several decades and includes an NEC multi-cathode source of negative ions by Cs sputtering, the ΔE-Q3D isotope separation system, and a multi-anode gas ionization chamber. The sensitivity of AMS mainly depends on its ability to suppress contamination. Given that the previous system alone could not achieve the required sensitivity for detecting ^{60}Fe, a Wien filter was installed after the accelerator magnetic systems to purify the beam and improve its sensitivity. The new setup was tested for ^{60}Fe measurements using a sample with ^{60}Fe/Fe at the level of 1.125×10^{-10}. The results demonstrated the following: Nearly all the contaminants in the beam of ^{60}Fe were effectively separated. The sensitivity of ^{60}Fe measurements with 5.8 h blank sample measurements at the AMS facility was evaluated to be better than 4.3×10^{-14}. For the lunar sample measurements, the duration would be approximately a few hundred hours. Thus, the sensitivity could in principle be expected to reach the level of 10^{-15}. Furthermore, the ion source and transmission efficiencies of the tandem accelerator did not achieve the best performance during the test experiment. Therefore, the sensitivity could be enhanced through further improvements in the future.

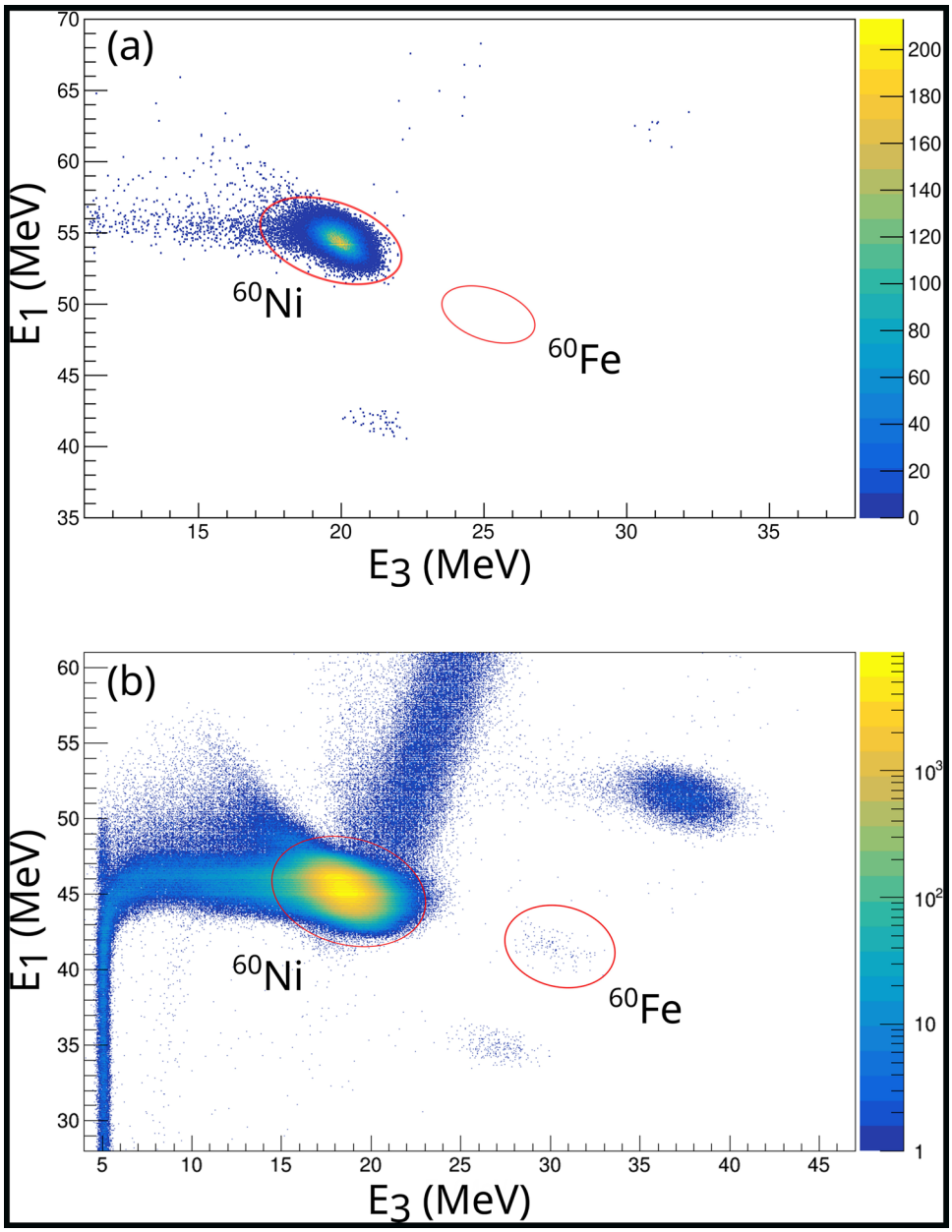

Fig. 3 (Color online) Two-dimensional spectra of E_1 versus E_3. **a** Spectrum measured with a blank sample. **b** Spectrum measured with the ^{60}Fe sample. It is noted that the pressure of the detector during the blank sample measurements was different from that of the ^{60}Fe sample measurements. Therefore, the energy ranges of Fig. 3a and b are not identical. The areas for ^{60}Fe and its isobar ^{60}Ni are marked by red circles

Table 2 Optimized accelerator parameters for ^{60}Fe measurements

Parameter	Value	Parameter	Value
Isotope	^{60}Fe	Material of cathode	Fe_2O_3 + Cu (1:1 by wt.)
Negative ion	$^{60}FeO^-$	Terminal voltage	11 MV
Accelerator stripper	Carbon foil (3 μg/cm^2)	Charge state/stripping yield	11/~ 7%
Wien filter voltage	±50 kV	Wien filter magnet	B = 0.092 T
Degrader	Si_3N_4 (1 μm)	Detector medium gas	Isobutane (35 mbar)

Acknowledgements The authors thank the staff of the HI-13 tandem accelerator for smooth operation of the machine.

Author contributions All authors contributed to the study conception and design. Yong-Shou Chen, Wei-Ping Liu, Bing Guo, Sheng-Quan Yan, Yun-Ju Li, You-Bao Wang, Zhi-Hong Li, Yang-Ping Shen and Ming He contributed to the conceptualization and methodology. Material preparation, data collection and analysis were performed by Yang Zhang, Sheng-Quan Yan, Ming He, Qing-Zhang Zhao, Wen-Hui Zhang, Chao-Xin Kan, Jian-Ming Zhou, Kang-Ning Li, Xiao-Fei Wang, Jian-Cheng Liu, Zhao-Hua Peng, Zhuo Liang, Ai-Ling Li, Jian Zheng, Qi-Wen Fan, Ding Nan, Wei Nan, Yu-Qiang Zhang,

Jia-Ying-Hao Li, Jun-Wen Tian, Jiang-Lin Hou, Chang-Xin Guo, Zhi-Cheng Zhang, Ming-Hao Zhu, Yu-Wen Chen, Yu-Chen Jiang, Tao Tian, Jin-Long Ma, Yi-Hui Liu, Jing-Yu Dong, Run-Long Liu and Mei-Yue-Nan Ma. The first draft of the manuscript was written by Yang Zhang and all authors commented on previous versions of the manuscript. All authors read and approved the final manuscript.

Data availability The data that support the findings of this study are openly available in Science Data Bank at https://cstr.cn/31253.11.sciencedb.j00186.00511 and https://doi.org/10.57760/sciencedb.j00186.00511.

Declarations

Conflict of interest The authors declare that they have no conflict of interest.

References

1. J.F. Snape, A.A. Nemchin, M.J. Whitehouse et al., The timing of basaltic volcanism at the Apollo landing sites. Geochim. Cosmochim. Ac. **266**, 29–53 (2019). https://doi.org/10.1016/j.gca.2019.07.042
2. D. Stöffler, G. Ryder, Stratigraphy and isotope ages of lunar geologic units: Chronological standard for the inner solar system. Space Sci. Rev. **96**, 9–54 (2001). https://doi.org/10.1023/A:1011937020193
3. H. Hiesinger, J.W. Head III., New views of lunar geoscience: an introduction and overview. Rev. Mineral. Geochem. **60**, 1–81 (2006). https://doi.org/10.2138/rmg.2006.60.1
4. L.E. Borg, J.N. Connelly, M. Boyet et al., Chronological evidence that the Moon is either young or did not have a global magma ocean. Nature **477**, 70–72 (2011). https://doi.org/10.1038/nature10328
5. H.-C. Tian, C. Zhang, W. Yang et al., Surges in volcanic activity on the Moon about two billion years ago. Nat. Commun. **14**, 3734 (2023). https://doi.org/10.1038/s41467-023-39418-0
6. C.L. Li, H. Hu, M.-F. Yang et al., Characteristics of the lunar samples returned by the Chang'E-5 mission. Nat. Sci. Rev. **9**, nwab188 (2022). https://doi.org/10.1093/nsr/nwab188
7. A. Wallner, M. Bichler, K. Buczak et al., Settling the half-life of ^{60}Fe: fundamental for a versatile astrophysical chronometer. Phys. Rev. Lett. **114**, 041101 (2015). https://doi.org/10.1103/PhysRevLett.114.041101
8. K.M. Ostdiek, T.S. Anderson, W.K. Bauder et al., Activity measurement of ^{60}Fe through the decay of ^{60m}Co and confirmation of its half-life. Phys. Rev. C **95**, 055809 (2017). https://doi.org/10.1103/PhysRevC.95.055809
9. C. Domingo-Pardo, I. Dillmann, T. Faestermann et al., S-process nucleosynthesis in massive stars: new results on ^{60}Fe,^{62}Ni and ^{64}Ni. AIP Conf. Proc. **1090**, 230–237 (2009). https://doi.org/10.1063/1.3087019
10. S.Q. Yan, X.Y. Li, K. Nishio et al., The ^{59}Fe (n,γ) ^{60}Fe cross section from the surrogate ratio method and its effect on the ^{60}Fe nucleosynthesis. Astrophys. J. **919,** 84 (2021). https://doi.org/10.3847/1538-4357/ac12ce
11. M. Limongi, A. Chieffi, The nucleosynthesis of ^{26}Al and ^{60}Fe in solar metallicity stars extending in mass from 11 to 120 M$\odot$: The hydrostatic and explosive contributions. Astrophys. J. **647**, 483 (2006). https://doi.org/10.1086/505164
12. L. Fimiani, D.L. Cook, T. Faestermann et al., Interstellar ^{60}Fe on the surface of the moon. Phys. Rev. Lett. **116**, 151104 (2016). https://doi.org/10.1103/PhysRevLett.116.151104
13. K. Knie, G. Korschinek, T. Faestermann et al., Indication for supernova produced ^{60}Fe activity on earth. Phys. Rev. Lett. **83**, 18–21 (1999). https://doi.org/10.1103/PhysRevLett.83.18
14. A. Wallner, J. Feige, N. Kinoshita et al., Recent near-earth supernovae probed by global deposition of interstellar radioactive ^{60}Fe. Nature **532**, 69–72 (2016). https://doi.org/10.1038/nature17196
15. C. Fitoussi, G.M. Raisbeck, K. Knie et al., Search for supernova-produced ^{60}Fe in a marine sediment. Phys. Rev. Lett. **101**, 121101 (2008). https://doi.org/10.1103/PhysRevLett.101.121101
16. D. Koll, G. Korschinek, T. Faestermann et al., Interstellar ^{60}Fe in Antarctica. Phys. Rev. Lett. **123**, 072701 (2019). https://doi.org/10.1103/PhysRevLett.123.072701
17. S. Hu, H. He, J. Ji et al., A dry lunar mantle reservoir for young mare basalts of Chang'e-5. Nature **600**, 49–53 (2021). https://doi.org/10.1038/s41586-021-04107-9
18. Q.-L. Li, Q. Zhou, Y. Liu et al., Two-billion-year-old volcanism on the moon from Chang'e-5 basalts. Nature **600**, 54–58 (2021). https://doi.org/10.1038/s41586-021-04100-2
19. H.-C. Tian, H. Wang, Y. Chen et al., Non-KREEP origin for Chang'e-5 basalts in the Procellarum KREEP Terrane. Nature **600**, 59–63 (2021). https://doi.org/10.1038/s41586-021-04119-5
20. X. Zeng, X. Li, J. Liu, Exotic clasts in Chang'e-5 regolith indicative of unexplored terrane on the Moon. Nat. Astron. **7**, 152–159 (2023). https://doi.org/10.1038/s41550-022-01840-7
21. Y. Yao, C. Xiao, P. Wang et al., Instrumental neutron activation analysis of Chang'E-5 lunar regolith samples. J. Am. Chem. Soc. **144**, 5478–5484 (2022). https://doi.org/10.1021/jacs.1c13604
22. Y. Jiang, J. Kang, S. Liao et al., Fe and Mg isotope compositions indicate a hybrid mantle source for Young Chang'E 5 mare basalts. Astrophys. J. Lett. **945**, L26 (2023). https://doi.org/10.3847/2041-8213/acbd31
23. Y. Yao, C. Xiao, L. Zhao et al., Determination of ^{58}Fe/^{54}Fe isotope ratios in Chang'E-5 lunar regolith by instrumental neutron activation analysis. Nucl. Anal. **3**, 100102 (2024). https://doi.org/10.1016/j.nucana.2024.100102
24. X. Lu, J. Chen, Z. Ling et al., Mature lunar soils from Fe-rich and young mare basalts in the Chang'e-5 regolith samples. Nat. Astron. **7**, 142–151 (2023). https://doi.org/10.1038/s41550-022-01838-1
25. K.N. Li, C.X. Kan, X.F. Wang et al., Practice and innovation in the operation and maintenance of HI-13 tandem acceleratorfor 35 years. Nuclear Techniques (in Chinese) **46**, 080005 (2023). https://doi.org/10.11889/j.0253-3219.2023.hjs.46.080005
26. W.P. Liu, Review of the development of tandem accelerator laboratory in 35 years. Nuclear Techniques (in Chinese) **46**, 080022 (2023). https://doi.org/10.11889/j.0253-3219.2023.hjs.46.080022
27. M. He, S. Jiang, S. Jiang et al., Development of AMS measurements and applications at the CIAE. Nucl. Instrum. Meth. Phys. Res. Sect. B **172**, 87–90 (2000). https://doi.org/10.1016/S0168-583X(00)00370-0
28. Y.L. Dou, M. Lin, M. He et al., AMS measurement of in-situ produced cosmogenic ^{10}Be in Loess Quartz in Luochuan. Chinese Phys. C **32** 279–283 (2008). http://csnsdoc.ihep.ac.cn/article/id/en/article/id/3152caed-097e-411e-8a82-c7c4e7ac8fb2
29. J. Gong, C. Li, W. Wang et al., 32Si AMS measurement with Δ E-Q3D method. Nucl. Instrum. Meth. Phys. Res. Sect. B **269**, 2745–2749 (2011). https://doi.org/10.1016/j.nimb.2011.08.026
30. C. Li, M. He, W. Zhang et al., AMS measurement of ^{36}Cl with a Q3D magnetic spectrometer at CIAE. Plasma Sci. Technol **14**, 543 (2012). https://doi.org/10.1088/1009-0630/14/6/25

31. K.J. Dong, M. He, S.Y. Wu et al., Application of ^{41}Ca tracer and its AMS measurement in CIAE. Chinese Phys. Lett. **21**, 51 (2004). https://doi.org/10.1088/0256-307X/21/1/015
32. Z.C. Li, Y.H. Cheng, Y. Chen et al., Beijing Q3D magnetic spectrometer and its applications. Nucl. Instrum. Meth. Phys. Res. Sect. A **336**, 150–161 (1993). https://doi.org/10.1016/0168-9002(93)91091-Z
33. C. Li, M. He, S. Jiang et al., An isobar separation method with Q3D magnetic spectrometer for AMS. Nucl. Instrum. Meth. Phys. Res. Sect. A **622**, 536–541 (2010). https://doi.org/10.1016/j.nima.2010.07.065
34. Y. Zhang, M. He, F. Wang et al., Developing the measurement of ^{60}Fe with AMS at CIAE. Nucl. Instrum. Meth. Phys. Res. Sect. B **438**, 156–161 (2019). https://doi.org/10.1016/j.nimb.2018.05.020
35. F.F. Wang, M. He, Y.X. Zhang et al., ^{60}Fe Sample preparation and extraction method for measurement with accelerator mass spectrometry. J. Isotopes **32**, 103 (2019). https://doi.org/10.7538/tws.2018.youxian.008. (**in Chinese**)